Tree Physiology 28, 1609–1617

Constraints on physiological function associated with branch architecture and wood density in tropical forest trees

FREDERICK C. MEINZER,[1,2] PAULA I. CAMPANELLO,[3] JEAN-CHRISTOPHE DOMEC,[4] M. GENOVEVA GATTI,[3] GUILLERMO GOLDSTEIN,[3,5] RANDOL VILLALOBOS-VEGA[5] and DAVID R. WOODRUFF[1]

[1] *USDA Forest Service, Pacific Northwest Research Station, Corvallis, OR 97331, USA*

[2] *Corresponding author (fmeinzer@fs.fed.us)*

[3] *Laboratorio de Ecología Funcional, Departamento de Ecología, Genética y Evolución, Facultad de Ciencias Exactas y Naturales, Universidad de Buenos Aires, Buenos Aires (C1428EHA), Argentina*

[4] *Department of Forestry and Environmental Resources, North Carolina State University, Raleigh, NC 27695, USA*

[5] *Department of Biology, University of Miami, Coral Gables, FL 33124, USA*

Received June 3, 2008; accepted August 1, 2008; published online September 2, 2008

Summary This study examined how leaf and stem functional traits related to gas exchange and water balance scale with two potential proxies for tree hydraulic architecture: the leaf area:sapwood area ratio (A_L:A_S) and wood density (ρ_w). We studied the upper crowns of individuals of 15 tropical forest tree species at two sites in Panama with contrasting moisture regimes and forest types. Transpiration and maximum photosynthetic electron transport rate (ETR_{max}) per unit leaf area declined sharply with increasing A_L:A_S, as did the ratio of ETR_{max} to leaf N content, an index of photosynthetic nitrogen-use efficiency. Midday leaf water potential, bulk leaf osmotic potential at zero turgor, branch xylem specific conductivity, leaf-specific conductivity and stem and leaf capacitance all declined with increasing ρ_w. At the branch scale, A_L:A_S and total leaf N content per unit sapwood area increased with ρ_w, resulting in a 30% increase in ETR_{max} per unit sapwood area with a doubling of ρ_w. These compensatory adjustments in A_L:A_S, N allocation and potential photosynthetic capacity at the branch level were insufficient to completely offset the increased carbon costs of producing denser wood, and exacerbated the negative impact of increasing ρ_w on branch hydraulics and leaf water status. The suite of tree functional and architectural traits studied appeared to be constrained by the hydraulic and mechanical consequences of variation in ρ_w.

Keywords: capacitance, functional convergence, hydraulic architecture, osmotic potential, photosynthesis, transpiration, water potential.

Introduction

Because the integrity and efficiency of long-distance water transport are critical to the growth and survival of land plants, especially trees, fundamental features constraining hydraulic architecture are expected to play a dominant role in determining a broad range of functional traits. Whole-plant leaf area-specific conductance (K_l) is a higher order component of hydraulic architecture that integrates the hydraulic properties of the entire soil-to-leaf water transport pathway (Küppers 1984). As an index of the efficiency of water supply in relation to potential transpirational demand, K_l is expected to constrain stomatal control of leaf gas exchange and water balance (Meinzer 2002, Sperry et al. 2002), and a number of studies have reported a close coordination between K_l and leaf gas exchange both within (Meinzer and Grantz 1990, Hubbard et al. 2001) and across (Meinzer et al. 1995, Mencuccini 2003, Santiago et al. 2004, Campanello et al. 2008) species. Similarly, the leaf area to sapwood area ratio (A_L:A_S) is a tree architectural index of potential transpirational demand relative to water transport capacity and therefore a potential proxy for K_l (Andrade et al. 1998, Tausend et al. 2000, Bucci et al. 2005).

In diffuse-porous species, variation in wood density (ρ_w) should constrain stem hydraulics (Stratton et al. 2000) because ρ_w is an index of the balance between solid material and the relative cross-sectional area available for water transport. Plant functional traits shown to be inversely related to ρ_w include rates of leaf gas exchange (Bucci et al. 2004, Santiago et al. 2004), xylem-specific and leaf-specific conductivity (Stratton et al. 2000, Bucci et al. 2004, Santiago et al. 2004), minimum leaf water potential (Bucci et al. 2004, Santiago et al. 2004), leaf osmotic potential at the turgor loss point (Gartner and Meinzer 2005), xylem vulnerability to embolism and implosion (Hacke et al. 2001) and xylem hydraulic capacitance (Meinzer et al. 2003, Pratt et al. 2007, Scholz et al. 2007).

Because multi-species surveys involving measurement of hydraulics in intact, field-grown plants present a series of methodological and logistical difficulties associated with simultaneous measurements of water fluxes and their driving forces, both of which are rarely steady state (Goldstein et al. 1998, Andrade et al. 1998, Domec et al. 2007), the ability to

link higher order functional traits to tree architectural features and biophysical properties that are relatively simple to measure would be beneficial. Nevertheless, relatively few studies have examined the extent to which higher order functional traits and physiological regulatory behavior scale in a species-independent manner with basic structural and biophysical attributes that govern hydraulic architecture. Correlations among traits may not necessarily be indicative of the mechanisms driving the relationships, but comparisons of multiple relationships across a range of organization from the simplest physical traits to more complex functional traits are likely to suggest potential mechanisms underlying the scaling relationships observed.

We studied individuals of 15 tropical forest tree species at two sites in Panama with contrasting rainfall regimes and forest types to examine how a number of leaf, stem and branch level functional traits related primarily to gas exchange and water balance scale with A_L:A_S and ρ_w of upper canopy branches. For the reasons outlined above, A_L:A_S and ρ_w are potential surrogates for various aspects of tree hydraulic architecture that should provide a basis for drawing inferences concerning the mechanistic nature of the leaf- and branch-level scaling relationships observed. We hypothesized that scaling relationships would be driven by the impacts of variation in A_L:A_S and ρ_w on hydraulic architecture and water balance. Specifically, we expected to observe inverse relationships between A_L:A_S and indices of leaf gas exchange capacity because A_L:A_S is a potential architectural proxy for K_l. As such, increasing A_L:A_S would imply decreasing water supply in relation to demand. In addition, we predicted that xylem specific conductivity and hydraulic capacitance would be inversely related to ρ_w and that these inverse relationships would be associated with greater fluctuations in leaf water status in species with denser wood.

Materials and methods

Study sites and plant material

Data were collected during the dry seasons of 1994, 1996, 2000, 2001, 2003 and 2004 from two canopy cranes operated by the Smithsonian Tropical Research Institute (STRI) in the Republic of Panama. Each crane is equipped with a gondola suspended by cables from a rotating jib that allows access to about 0.8 ha of forest. One crane is located in an old-growth forest in the Parque Nacional San Lorenzo on the Caribbean side of the Isthmus of Panama, where mean annual precipitation is about 3100 mm. The other crane is located in a seasonally dry secondary forest in the Parque Natural Metropolitano near the edge of Panama City, which receives about 1800 mm of precipitation annually, with a distinct dry season between late December and April. The dry season at Parque San Lorenzo is shorter and less intense that at Parque Metropolitano. There is no overlap among tree species between the two sites. Seven individuals were studied at the Parque San Lorenzo site and eight at the Parque Metropolitano site representing a total of 15 species (Table 1).

Transpiration

The constant heating method described by Granier (1985) was used to measure transpiration (E) as sap flow through branches in the upper crowns of 12 species. For measurements in 1996, a pair of 20-mm-long, 2-mm-diameter temperature probes (UP GmbH, Munich, Germany) was installed in each of three to four replicate branches per tree. The upper (downstream) probe was continuously heated with a constant current power supply (UP GmbH), while the unheated upstream probe served as a temperature reference. For measurements in 2000, 2001 and 2004, variable length probes with a heated and

Table 1. Characteristics of the individual trees studied at two tropical forest sites in Panama.

Species	Family	Diameter (m)	Height (m)	A_L:A_S (m^2 cm^{-2})	Wood density (g cm^{-3})
Parque San Lorenzo					
Aspidosperma cruenta	Apocynaceae	0.29	29	1.16	0.74
Manilkara bidentata	Sapotaceae	0.66	30	0.61	0.67
Protium panamense	Burseraceae	0.28	16	0.58	0.62
Tachigalia versicolor	Fabaceae	0.31	23	1.19	0.64
Tapirira guianensis	Anacardiaceae	0.70	34	0.67	0.50
Trattinickia aspera	Burseraceae	0.37	24	0.64	0.57
Vochysia ferruginea	Vochysiaceae	0.42	26	0.72	0.56
Mean		0.43	26	0.80	0.61
Parque Metropolitano					
Anacardium excelsum	Anacardiaceae	0.98	38	0.51	0.39
Cecropia longipes	Cecropiaceae	0.20	18	0.34	0.33
Chrysophyllum cainito	Sapotaceae	0.33	23	0.90	0.66
Cordia alliodora	Boraginaceae	0.34	26	0.65	0.52
Ficus insipida	Moraceae	0.65	28	0.50	0.40
Luehea seemannii	Tiliaceae	0.75	24	0.58	0.48
Schefflera morototoni	Araliaceae	0.47	22	0.45	0.40
Spondias mombin	Anacardiaceae	0.33	23	0.39	0.38
Mean		0.51	25	0.54	0.44

reference sensor measuring length of 10 mm at the probe tip (James et al. 2002) were installed in three to five replicate branches per tree. All probes were shielded with a layer of foam insulation surrounded by an outer layer of reflective insulation. Concurrent differential voltage measurements across the copper thermocouple leads were converted to a temperature difference between the heated and reference sensor (ΔT). Signals from the sap flow probes were scanned every minute and 10-min means were recorded by a data logger equipped with a 32-channel multiplexer and stored in a solid-state storage module. Mass flow of sap was obtained by multiplying flow density by the sapwood area, which included the entire cross-sectional area of the xylem for the size range of branches in which probes were installed (3 to 6-cm-diameter). Leaf area distal to the probes ranged from 2 to 13 m^2 and was determined by multiplying the total number of leaves by the mean area per leaf obtained from a subsample of 50 to 200 leaves.

Photosynthetic capacity and leaf nitrogen content

Chlorophyll fluorescence was measured on 10 species during 2003 using a pulse-amplitude modulated yield analyzer (Mini-PAM, Waltz, Effeltrich, Germany). Saturation pulses were applied for 0.8 s at a photosynthetic photon flux (PPF) of 3500 μmol m^{-2} s^{-1}. Measurements were made between predawn and midday in fully expanded and exposed sun leaves to minimize the impacts of any afternoon depression in photosynthetic capacity or photoinhibition associated with acclimation to shade. Quantum yields of PS II were obtained for the complete range of PPF values experienced by plants (0 to 2000 μmol m^{-2} s^{-1}). Measurements of PPF were made with the Mini-PAM's micro-quantum sensor. A steady-state light response curve for each species was generated with leaves adapted to the PPF values measured in the field. Maximum fluorescence yield (F_m) and dark fluorescence yield (F_o) of PSII were recorded in predawn conditions to determine dark-adapted quantum yields ($F_v/F_m = F_m - F_o)/F_m$). Dark-adapted quantum yield corresponded to the initial points of the light curves. Steady-state fluorescence (F) and maximal fluorescence in the light-adapted state (F_m') of PSII were measured for different PPF values. Values of electron transport rates (ETR) through PSII were obtained from quantum yield ($\Delta F/F_m' = (F_m' - F)/F_m'$):

$$\mathrm{ETR} = (\Delta F/F_m')\, I\, \alpha\, 0.5 \quad (1)$$

where I is the incident PPF, and α is leaf absorbance. The 0.5 factor assumes an even distribution of absorbed quanta between PSII and PSI so two photons are required per electron passed through PSII. The ETR correction factor "α" takes into account that only a fraction of incident light is absorbed by the two photosystems. A value of $\alpha = 0.84$ was used for calculations (Ehleringer 1981, Björkman and Demmig 1987).

The photosynthetic capacity expressed as the maximum electron transport rate (ETR_{max}; μmol electrons m^{-2} s^{-1}) was calculated from light curves using the asymptotic exponential equation:

$$y = (\mathrm{ETR}_{max})\,(1 - e^{-bx}) \quad (2)$$

where y is photosynthetic rate, x is irradiance and b is the instantaneous fractional growth rate of the exponential function (Rascher et al. 2000). Curve fits obtained with this equation yielded r^2 values ranging from 0.87 to 0.99, consistent with the absence of significant photoinhibition.

Foliage on which chlorophyll fluorescence was measured was collected, dried and ground and analyzed for N content on a Carlo Erba elemental analyzer (NC 2500, CE Elantech, Lakewood, NJ). For the remaining five species, total N content of fully exposed upper canopy leaves was determined by the micro-Kjeldahl method. Leaf mass per area (LMA) was determined on a minimum of five leaves per species.

Leaf water relations

The water potential of upper-canopy leaves (Ψ_L) of nine species was determined with a pressure chamber (PMS Instrument Company, Albany, OR) near midday on clear dry days during the dry season. At each sampling time, measurements were obtained from three to five leaves of each tree. Balance pressures were determined either in the canopy crane gondola immediately after leaf excision, or the leaves were sealed in plastic bags and dropped to the base of the crane for determination of balance pressures within 10 min of excision.

The pressure–volume technique (Tyree and Hammel 1972) was used to assess bulk leaf osmotic potential at zero turgor ($\Psi_{\pi z}$) and leaf capacitance (C) in nine of the species. Portions of terminal branches were excised in the upper canopy and their bases immediately recut under water. The cut ends remained under water with the terminal leafy portions enclosed in a plastic bag to allow partial rehydration during transit from the canopy crane to the laboratory. Individual leaves or leafy shoots were used for pressure–volume analyses depending on petiole length and leaf size. Pressure–volume curves were initiated by first determining the fresh mass of the sample, then measuring its water potential with a pressure chamber. Alternate measurements of fresh mass and Ψ_L were repeated during slow dehydration on the laboratory bench until Ψ_L approached the measuring range of the pressure chamber (–4 MPa). We tested for rehydration-induced artifacts previously reported for some woody species (Bowman and Roberts 1985, Meinzer et al. 1986, Evans et al. 1990) by comparing pressure–volume curves obtained from samples at different levels of initial hydration and found none. The transition point between the nonlinear and linear portions of the curve was taken to be the bulk tissue osmotic potential at zero turgor. Bulk leaf C was determined from the slope of the relationship between relative water content and Ψ_L obtained from pressure–volume curves at values of Ψ_L less negative than $\Psi_{\pi z}$. Values of osmotic potential and C reported here are means from three to five curves per species.

Stem water relations

Moisture release curves for sapwood of terminal branches were determined for ten species according to the method de-

scribed by Meinzer et al. (2003). Briefly, small cylinders of sapwood were allowed to hydrate in distilled water overnight and then quickly blotted to remove excess water, placed in the caps of thermocouple psychrometer chambers (83 Series, JRD Merrill Specialty Equipment, Logan, UT), weighed, and sealed inside the rest of the chamber for determination of Ψ isotherms. Each chamber contained three cylindrical tissue samples. The psychrometer chambers were placed in an insulated water bath and allowed to equilibrate for 2 to 3 h before measurements were started with a 12-channel digital psychrometer meter (85 Series, JRD Merrill Specialty Equipment). Measurements were repeated at 30-min intervals until the Ψ values stabilized. The chambers were opened and the samples were allowed to dehydrate for different time intervals, reweighed in the psychrometer caps, resealed inside the psychrometer chambers and allowed to equilibrate for another determination of Ψ. Moisture release curves were generated by plotting sapwood Ψ against relative water deficit. Data points from three to four replicate curves per species were pooled. Species-specific values of sapwood C (kg m^{-3} MPa^{-1}) were taken as the slopes of linear regressions fitted to the initial phase of moisture release curves plotted as the cumulative mass of water released against sapwood Ψ (Meinzer et al. 2003). Mass of water per unit sapwood volume at saturation (kg m^{-3}) was calculated by multiplying the saturated/dry mass ratio by sapwood density (kg m^{-3}) and subtracting sapwood density. The cumulative mass of water released per unit sapwood volume was then calculated by multiplying the tissue relative water deficit at a given value of sapwood Ψ by the mass of water per unit sapwood volume at saturation. Density was determined for small cylinders of sapwood collected as described above. Volume displacement was determined for samples of saturated tissue, which were oven dried for determination of mass.

Maximum specific conductivity (k_s) was determined for segments of terminal branches 2–5 cm in diameter and greater than 35 cm in length excised near the top of the canopy. After excision, the branches were immediately recut under water in the crane gondola and transported to the laboratory for measurement. In the laboratory, a 15 to17-cm-long section of each branch (0.7 to 1.2 cm in diameter) was cut and both ends were smoothed with clean razor blades. The stem segments were then sealed into a double-ended pressure chamber with both ends protruding and attached with tubing to an apparatus for measuring hydraulic conductivity (k_h). The downstream end of the segment was connected to a 1-ml graduated pipette and the upstream end of the segment was attached to tubing connected to a reservoir of filtered water (0.22 um) that was pressurized at 0.15 MPa for 40 min to remove emboli and restore the segment to its maximum conductivity. The pressure was then lowered to 5.5 kPa and the chamber was pressurized to 0.05 MPa to prevent extrusion of water from leaf scars during measurement of axial flow. When flow had stabilized, the time required for the meniscus in the pipette to cross five consecutive graduation marks (0.5 ml) was recorded. Maximum k_h was calculated as the mass flow rate through the segment divided by the pressure gradient (MPa m^{-1}) across the segment. Conductivity was divided by the xylem cross-sectional area to obtain k_s and by the leaf area distal to the segment to obtain leaf-specific conductivity (k_l). Conductivity data reported here are means of values obtained from five to six stem segments per species. Following conductivity measurements, xylem density was determined as described above.

The water potential of terminal branches (Ψ_{br}) was estimated with a pressure chamber from balance pressures of covered, non-transpiring leaves (Meinzer et al. 2003). Leaves were enclosed in aluminum foil and plastic bags in the afternoon before the day of measurements. At each sampling time, measurements were obtained from three to five leaves of each tree as described above for exposed leaves.

Statistical analysis

Trends in sapwood area-based ETR_{max} and E with ρ_w (Figure 5b) were modeled by first using the regression fitted to the relationship between A_L:A_S and ρ_w ($y = 1.60x - 0.18$; Figure 5a). The corresponding values of A_L:A_S were then used in the regression equations developed for the data in Figures 1 and 2a to obtain values of E ($y = 0.42 + 36.54e^{(-8.96x)}$) and ETR_{max} ($\log(y) = 1.95 - 0.78\log(x)$), which were multiplied by A_L:A_S to convert from a unit leaf area basis to a branch sapwood area basis. These estimates were then normalized to values at a ρ_w of 0.3 g cm^{-3}, which corresponded roughly to the lowest ρ_w among the species studied. Pearson correlations were used to analyze relationships between functional traits and A_L:A_S or ρ_w after log transformation of data. Significance levels of least squares regressions were assessed by ANOVA. Differences in A_L:A_S and ρ_w among sites were evaluated by one-way ANOVA with site as the main factor. Differences in the dependence of sapwood C on ρ_w among sites were assessed by one-way ANCOVA after confirming homogeneity of the regressions for the two sites ($F = 0.64$, $P = 0.45$).

Results

Values of branch A_L:A_S and ρ_w varied widely among the 15 trees studied (Table 1). Branch A_L:A_S was higher at the wetter San Lorenzo site than at the drier and more seasonal Parque Metropolitano ($P = 0.04$). Mean ρ_w was also significantly greater ($P = 0.004$) for the trees studied at the Parque San Lorenzo site. Mean basal diameter and height of the trees selected for study were similar across the two sites. Nine of the 12 leaf and stem functional traits examined were significantly correlated with A_L:A_S or ρ_w across species (Table 2).

Several scaling relationships of leaf functional traits with tree architecture and ρ_w were identified. Transpiration per unit leaf area declined sharply with increasing A_L:A_S for the 12 species in which upper-branch sap flow was measured as a proxy for transpiration (Figure 1). Consistent with the behavior of transpiration, ETR_{max}, an index of photosynthetic capacity, and the ratio of ETR_{max} to leaf N content (ETR_{max}/N), an index of instantaneous photosynthetic nitrogen-use efficiency, also declined with increasing A_L:A_S ($P < 0.0001$ and $P = 0.003$, respectively; Figure 2). The inverse relationship between ETR_{max}/N and A_L:A_S was not associated with significant trends

in leaf N content on a mass or area basis with variation in A_L:A_S or ρ_w (Table 2 and data not shown).

Both midday leaf water potential (Ψ_L) and the bulk leaf osmotic potential at zero turgor ($\Psi_{\pi z}$) declined linearly with increasing ρ_w (P = 0.0003 and 0.004, respectively, Figure 3a). Variation in ρ_w explained about 84% of the variation in Ψ_L. The slopes of the regression lines were not statistically different, implying that minimum values of bulk leaf turgor were similar across species when the daily minimum value of Ψ_L was attained. The specific conductivity of branch sapwood (k_s) decreased exponentially from a maximum value of about 12 kg m^{-1} s^{-1} MPa^{-1} when branch ρ_w was 0.4 g cm^{-3} to a minimum value of 1.6 kg m^{-1} s^{-1} MPa^{-1} when ρ_w was 0.74 g cm^{-3} (Figure 3b). Species from both sites appeared to share a common relationship between k_s and ρ_w. However, k_s was not significantly correlated with A_L:A_S (Table 2). Consistent with the relationship between k_s and ρ_w, k_l decreased exponentially with ρ_w (Figure 3c). Sapwood C also declined sharply with increasing ρ_w (Figure 4a), but distinct site-specific relationships appeared to exist with species occurring at the wetter forest site having greater values of sapwood C at a given value of ρ_w (F = 40.6, P = 0.0004). Maximum values of C were similar (~400 kg m^{-3} MPa^{-1}) at both sites. Bulk leaf C on a mass basis was inversely related to ρ_w (P = 0.004) with species from both sites appearing to share a common relationship (Figure 4b).

The leaf area to sapwood area ratio of upper-canopy branches increased about threefold with a doubling of ρ_w (Figure 5a). Although a single linear regression fitted to data from both sites was highly significant (r^2 = 0.66, P = 0.0002), the re-

Table 2. Correlation coefficients and their statistical significance for comparisons of leaf and stem functional traits with branch architecture and sapwood density. Traits with negative values (Ψ_{br}, Ψ_L, $\Psi_{\pi z}$) were converted to positive values for log transformation, but signs of correlation coefficients reflect correlations for untransformed data. Abbreviations: * P < 0.05, ** P < 0.01, *** P < 0.001.

Trait	n	A_L:A_S	Wood density
Leaf			
E_{max}	12	−0.82 ***	−0.47 ***
ETR_{max}	10	−0.97 ***	−0.62
ETR/N	10	−0.83 **	−0.64 *
%N	15	0.20	0.41
LMA	15	0.21	0.51 *
Ψ_L	9	−0.51	−0.93 ***
$\Psi_{\pi z}$	9	−0.22	−0.85 **
C	9	−0.58	−0.93 ***
Stem			
k_s	10	−0.46	−0.83 **
k_l	10	−0.67 *	−0.89 ***
Ψ_{br}	10	−0.30	−0.38
C	10	0.04	−0.40

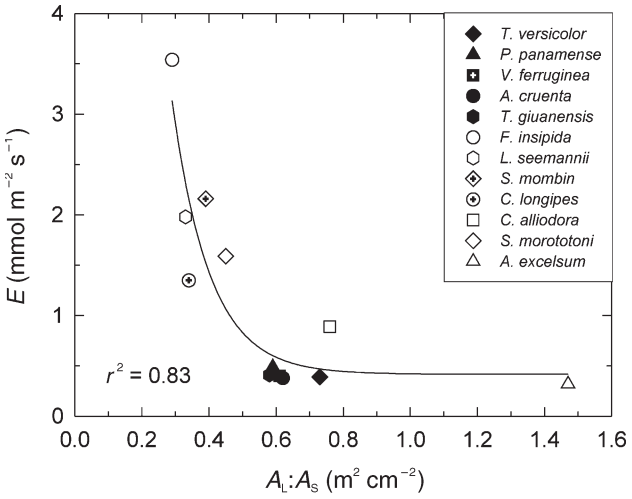

Figure 1. Maximum branch transpiration rate per unit leaf area (E) in relation to leaf area:sapwood area ratio (A_L:A_S) for upper crown branches of 12 Panamanian forest tree species growing in two sites with different rainfall regimes and forest types. Values are means of three to five branches per tree. Open symbols, drier site; closed symbols wetter site.

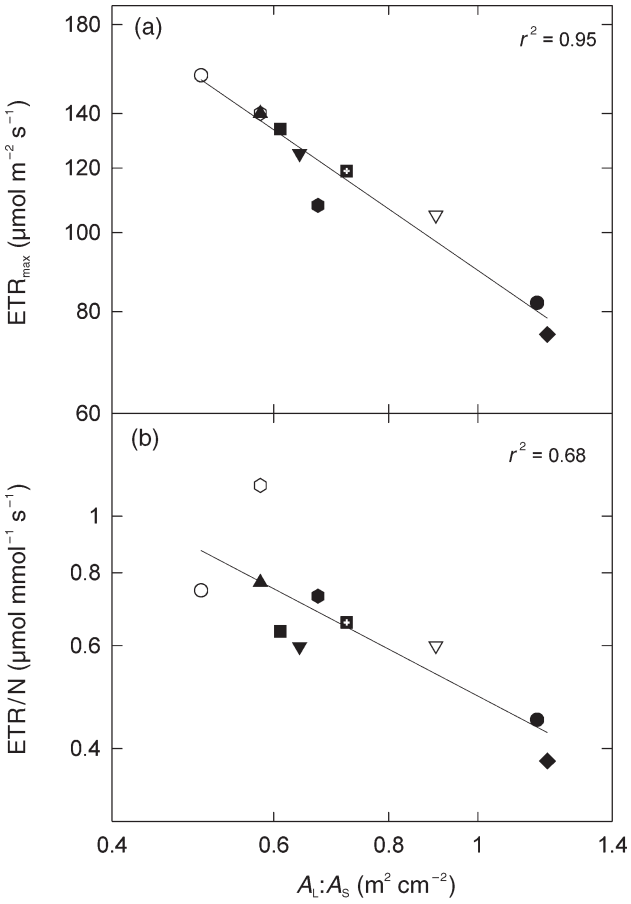

Figure 2. Log–log plots of (a) maximum photosynthetic electron transport rate per unit leaf area (ETR_{max}) and (b) maximum electron transport rate per unit leaf nitrogen (ETR/N) in relation to the branch leaf area:sapwood area ratio (A_L:A_S) for 10 Panamanian forest tree species. Symbols: (▽) *Chrysophllum cainito*, (■) *Manilkara bidentata*, (▼) *Trattinickia aspera*, remaining symbols as in Figure 1.

lationship for the trees studied at the drier Parque Metropolitano site was much less variable (r^2 = 0.97, P < 0.0001). Scaling of transpiration on a unit branch sapwood area basis with ρ_w reduced transpiration by about 20% over the range of ρ_w observed (Figure 5b). In contrast, scaling photosynthetic capacity (ETR_{max}) per branch sapwood area increased photosynthetic capacity by about 30% over the same range of ρ_w (Figure 5b). The total amount of foliar N per unit sapwood area increased from ~60 mmol N cm^{-2} sapwood area in the species with the lowest ρ_w to ~210 mmol N cm^{-2} in the species with the highest ρ_w (P = 0.0004, Figure 5c).

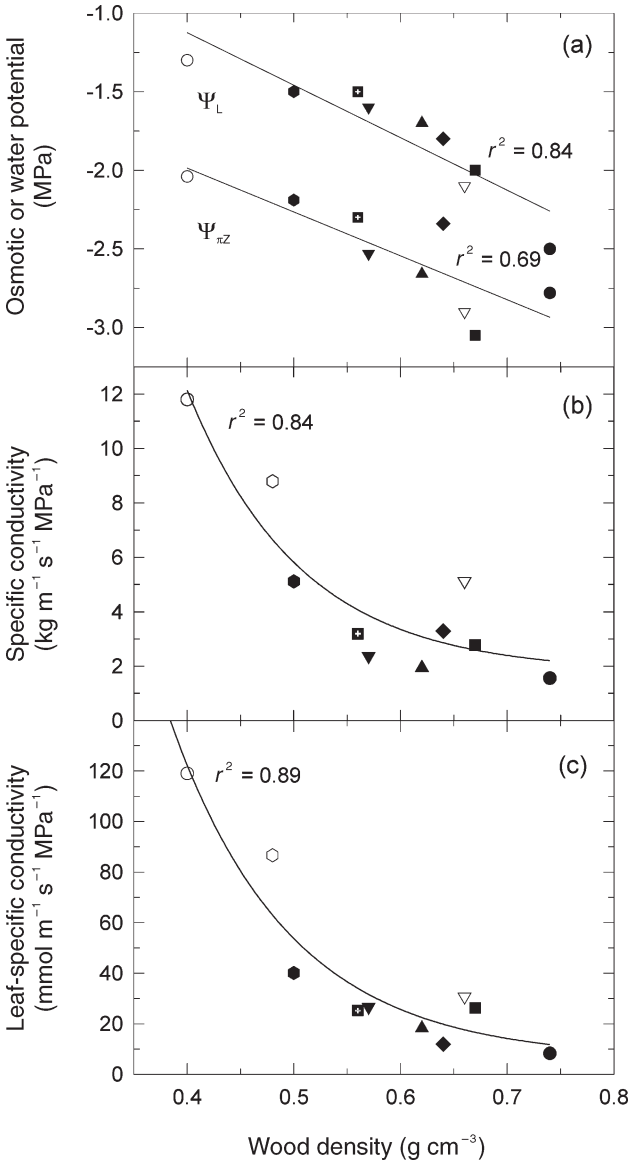

Figure 3. Leaf and stem functional traits in relation to branch wood density for Panamanian forest trees. (a) Mean daily minimum leaf water potential (Ψ_L) and bulk leaf osmotic potential at zero turgor ($\Psi_{\pi z}$) for nine species, (b) branch xylem specific conductivity for 10 species, (c) leaf-specific conductivity for the same species shown in (b). Symbols as in Figures 1 and 2.

Discussion

Simple tree architectural and wood physical properties (A_L:A_S and ρ_w) accounted for a large fraction of the variation in several leaf and stem functional traits among individuals and species growing at contrasting sites. As hypothesized, A_L:A_S appeared to be a reliable proxy for K_l, and ρ_w served as a proxy for k_s, C and their impact on leaf water relations. The scaling relationships found here have practical and theoretical implications for understanding and predicting emergent properties of complex multi-species ecosystems. These relationships obtained from data collected over multiple years on individuals growing in contrasting sites and representing different tree functional groups, are unlikely to be merely correlative, but imply direct or indirect mechanistic links between variables as we argue below.

Branch architectural constraints on leaf gas exchange

As a relative index of potential transpirational demand in relation to the hydraulic capacity of the xylem, A_L:A_S is an important component of tree hydraulic architecture. Results of a number of studies suggest that k_l scales uniformly with A_L:A_S among co-occurring species with A_L:A_S explaining 50% or more of the variation in k_l (Tausend et al. 2000, Bucci et al. 2005). Furthermore, adjustments in A_L:A_S have been shown to

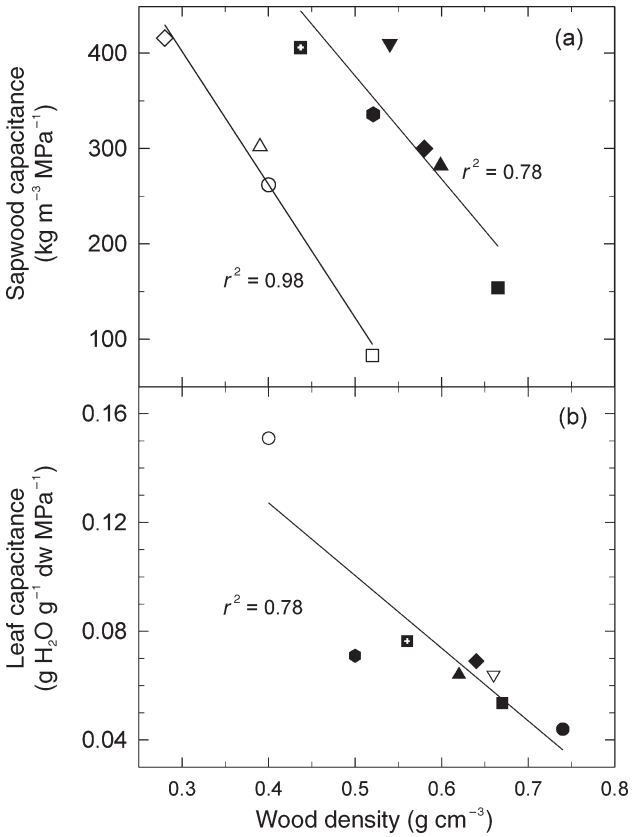

Figure 4. (a) Sapwood and (b) leaf capacitance in relation to wood density for several Panamanian forest tree species. Symbols as in Figures 1 and 2.

play a role in conserving k_l under a range of circumstances such as exposure to seasonal drought (Bucci et al. 2005) and pathogens that reduce xylem conductivity (Meinzer et al. 2004). The tendency for A_L:A_S to decrease with increasing tree height (McDowell et al. 2002*a*) can be interpreted as a compensatory response that maintains K_l as the length and tortuosity of the hydraulic path increase (McDowell et al. 2002*b*). Thus, A_L:A_S may be a reliable surrogate for K_l despite species-specific differences in sapwood specific conductivity. Because K_l is a major determinant of the relationship between E and Ψ_L, stomatal control of E is closely coordinated with variation in K_l (Meinzer and Grantz 1990, Meinzer et al. 1995, Hubbard et al. 2001), and therefore should be coordinated with

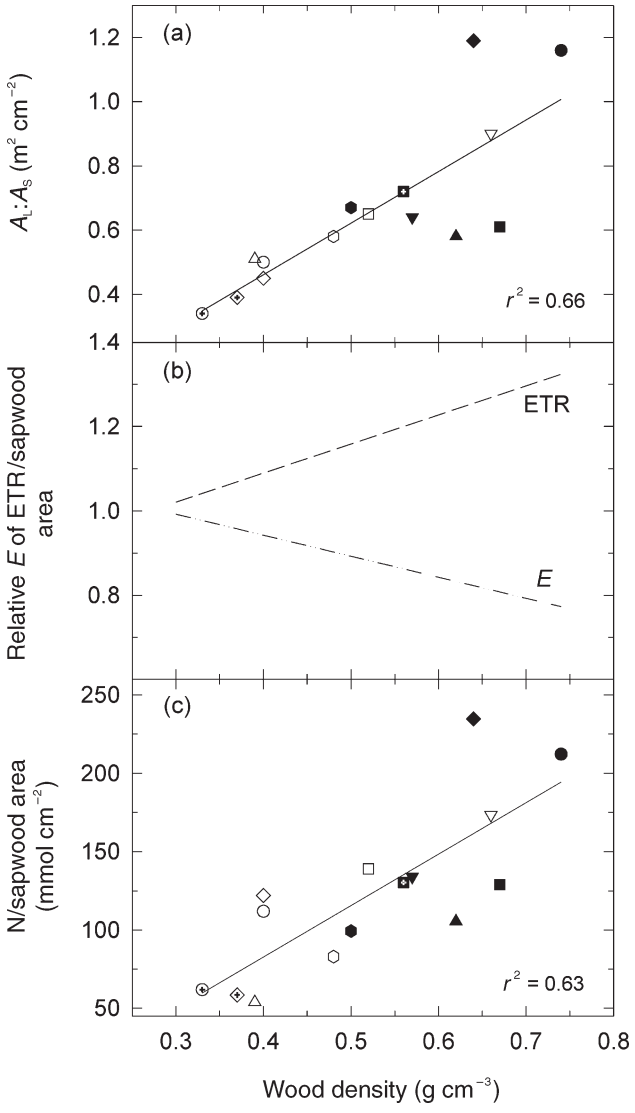

Figure 5. Branch-scale architectural and functional traits in relation to branch wood density for Panamanian forest tree species. (a) Leaf to sapwood area ratio (A_L:A_S). (b) Relative trends of maximum transpiration (E) and maximum photosynthetic electron transport rate (ETR_{max}) per unit branch sapwood area. (c) Total leaf N per unit sapwood area. Symbols as in Figures 1 and 2.

A_L:A_S. In agreement with this, E decreased by 94% as A_L:A_S increased five-fold from ~0.3 to 1.5 m^2 cm^{-2} (Figure 1). The dependence of E on A_L:A_S conformed with an exponential decay function, consistent with the exponential decline in k_l with increasing A_L:A_S (Tausend et al. 2000, Bucci et al. 2005). Estimates of E and A_L:A_S were not entirely independent in the present study because E was calculated by multiplying sap flux by branch sapwood area then normalizing by the leaf area distal to the sap flow sensors. Nevertheless, a previous study demonstrated that stomatal conductance scaled uniformly with independently measured k_l among 20 Panamanian forest tree species (Santiago et al. 2004) and in the present study k_l was significantly correlated with A_L:A_S (Table 2) among some of the same species.

Our results suggest that increasing A_L:A_S imposed a greater relative constraint on E than on photosynthetic capacity (ETR_{max}), which declined by about 50% as A_L:A_S increased from 0.5 to 1.2 m^2 cm^{-2} (Figure 2a). Over a similar range, E decreased by nearly 80%. Thus, relative stomatal limitation of photosynthesis, and therefore intrinsic water-use efficiency, should have increased as A_L:A_S increased. Potentially lower photosynthetic nitrogen-use efficiency in trees with greater A_L:A_S (Figure 2b) appeared to result largely from coordination of ETR_{max} with increased stomatal constraints on photosynthesis as there was no tendency for leaf N content to be higher in individuals with greater A_L:A_S (Table 2).

Wood density as a scalar of functional traits

Coordination between leaf water relations traits and ρ_w was likely mediated by the inverse relationship between sapwood k_s and ρ_w (Figure 3b). The relative xylem lumen volume available for water transport is inversely related to ρ_w and in diffuse-porous species having a relatively large fraction of vessels close to the hydraulic mean diameter, k_s should scale predictably with ρ_w (Stratton et al. 2000, Bucci et al. 2004). However, a trade-off between k_s and ρ_w is less likely in ring-porous species with few large vessels and a high density of fibers because k_s increases with the fourth power of vessel diameter. Leaf-specific conductivity also showed a strong negative correlation with ρ_w (Figure 3c, Table 2), implying lack of a compensatory decline in A_L:A_S constraining variation in k_l with increasing ρ_w. Rather, the roughly threefold increase in A_L:A_S with increasing ρ_w (Figure 5a) did not mitigate but amplified the negative impact of increasing ρ_w on hydraulic efficiency, causing the relative variation in k_l to be more than twice as great as that of k_s as ρ_w varied between 0.4 and 0.74 g cm^{-3} (cf. Figures 3b and 3c).

The positive relationship between A_L:A_S and ρ_w found here seems counterintuitive, but is consistent with the findings of Bucci et al. (2004) for six Brazilian savanna species and Wright et al. (2006) for species representing three Australian vegetation types. In contrast, negative associations between A_L:A_S and ρ_w have been reported for chaparral shrubs (Ackerly 2004) and several Floridian oak species (Cavender-Bares et al. 2004). The specific selective pressures responsible for these opposing scaling relationships have not been identified. In the

present study, the potential gain in photosynthetic capacity on a branch sapwood area basis associated with increasing ρ_w (Figure 5b) may have offset the negative impact of higher ρ_w on branch hydraulics (Figure 3b) and leaf water status (Figure 3a). The coexistence of species representing a broad range of ρ_w and A_L:A_S at the Parque Natural Metropolitano site (Figure 5a) suggests that in this early successional secondary forest, a particular combination of A_L:A_S and ρ_w may have neutral consequences for competitive ability. The prevalence of species with higher A_L:A_S and ρ_w at Parque San Lorenzo (Figure 5a) implies that this combination of branch architecture and mechanical strength may confer a competitive advantage in a mature forest.

The hydraulic consequences of variation in ρ_w were evident in the relatively large range in daily minimum Ψ_L from –1.4 MPa in *Ficus insipida* to –2.5 MPa in *Aspidosperma cruenta* (Figure 3a). The decline in Ψ_L with increasing ρ_w implies that stomatal coordination of E with k_l yielded a curvilinear relationship consistent with anisohydric regulation of minimum Ψ_L across species even though individual species may display isohydric behavior (Hubbard et al. 2001, Bucci et al. 2005, Fisher et al. 2006). Variation in $\Psi_{\pi z}$ with ρ_w paralleled that of minimum Ψ_L, suggesting that minimum turgor remained nearly constant at 0.7 to 0.8 MPa as ρ_w varied across species. Nevertheless, the positive correlation between LMA and ρ_w (Table 2) is suggestive of greater relative constraints on leaf expansion in species with denser wood. Scaling of Ψ_L and $\Psi_{\pi z}$ with ρ_w is consistent with earlier findings of strong constraints imposed by ρ_w on leaf water relations (Meinzer 2003, Bucci et al. 2004, Gartner and Meinzer 2005).

Inverse relationships between ρ_w and stem and leaf C (Figure 4) suggested additional hydraulic costs of increasing ρ_w. Given the role of capacitance in buffering diurnal variation in stem and leaf Ψ (Meinzer et al. 2003, 2008, Scholz et al. 2007), increasing ρ_w implies further stomatal restriction of E beyond that associated with reduced k_s to constrain variation in Ψ. The basis for the consistent difference in the relationship between sapwood C and ρ_w among individuals growing at the two sites (Figure 4a) was not determined. Depending on the relative contributions of the compartments from which water is withdrawn, the dependence of sapwood volumetric C on ρ_w may be determined largely by the osmotic and elastic properties of xylem parenchyma and by xylem vulnerability to embolism (Scholz et al. 2007, Meinzer et al. 2008).

Leaf versus branch level properties

Trends in a suite of tree functional and architectural traits appeared to be inextricably linked via the hydraulic and mechanical consequences of variation in ρ_w. The impact on k_l of the sharp decline in k_s with increasing ρ_w was amplified by a concurrent increase in A_L:A_S. Consequently, coordination of gas exchange with k_l led to sharp declines in leaf-level E and photosynthetic capacity with increasing A_L:A_S. Despite stomatal coordination of E with k_l, Ψ_L declined in a linear fashion with increasing ρ_w, which required increased allocation to osmotically active solutes to maintain turgor (Figure 3a) and likely contributed to increased leaf mass per area (Table 2).

However, the apparent consequences of higher ρ_w may depend on the scale at which functional traits are characterized. The negative hydraulic impacts of increasing ρ_w may have been partly offset by an associated increase in branch mechanical strength (van Gelder et al. 2006), permitting the display of a greater leaf area per branch cross-sectional area (A_L:A_S). At the branch level, the relative increases in A_L:A_S and allocation of N with increasing ρ_w were similar because leaf-level N content did not vary significantly with increasing A_L:A_S or ρ_w (Table 2). These parallel changes in A_L:A_S and N allocation were associated with a projected 30% increase in ETR_{max} on a branch sapwood area basis as ρ_w doubled (Figure 5b). Nevertheless, the compensatory adjustments in tree architecture and N allocation at the branch level were insufficient to completely offset the increased carbon and hydraulic costs of producing denser wood, consistent with slower growth rates of tropical trees with dense wood (Suzuki 1999, Muller-Landau 2004).

Acknowledgments

This research was supported by National Science Foundation Grant IBN 99-05012 to F. Meinzer and G. Goldstein. We thank the Smithsonian Tropical Research Institute for providing facilities and logistical support, and the expertise of the canopy crane operators.

References

Ackerly, D. 2004. Functional strategies of chaparral shrubs in relation to seasonal water deficit and disturbance. Ecol. Monogr. 74:25–44.

Andrade, J.L., F.C. Meinzer, G. Goldstein, N.M. Holbrook, J. Cavelier, P. Jackson and K. Silvera. 1998. Regulation of water flux through trunks, branches and leaves in trees of a lowland tropical forest. Oecologia 115:463–471.

Björkman, O. and B. Demmig. 1987. Photon yield of O_2 evolution and chlorophyll fluorescence characteristics at 77 K among vascular plants of diverse origins. Planta 170:489–504.

Bowman, W.D. and S.W. Roberts. 1985. Seasonal changes in tissue elasticity in chaparral shrubs. Physiol. Plant. 65:233–236.

Bucci, S.J., G. Goldstein, F.C. Meinzer, F.G. Scholz, A.C. Franco and M. Bustamante. 2004. Functional convergence in hydraulic architecture and water relations of tropical savanna trees: from leaf to whole plant. Tree Physiol. 24:891–899.

Bucci, S.J., G. Goldstein, F.C. Meinzer, A.C. Franco, P. Campanello and F.G. Scholz. 2005. Mechanisms contributing to seasonal homeostasis of minimum leaf water potential and predawn disequilibrium between soil and plant water potential in Neotropical savanna trees. Trees 19:296–304.

Campanello, P.I., M.G. Gatti and G. Goldstein. 2008. Coordination between water-transport efficiency and photosynthetic capacity in canopy tree species at different growth irradiances. Tree Physiol. 28:85–94.

Cavender-Bares, J., K. Kitajima and F.A. Bazzaz. 2004. Multiple trait associations in relation to habitat differentiation among 17 Floridian oak species. Ecol. Monogr. 74:635–662.

Domec, J.-C., F.C. Meinzer, B. Lachenbruch and J. Housset. 2007. Dynamic variation in sapwood specific conductivity in six woody species. Tree Physiol. 27:1389–1400.

Ehleringer, J. 1981. Leaf absorptances of Mohave and Sonoran desert plants. Oecologia 49:366–370.

Evans, R.D., R.A. Black and S.O. Link. 1990. Rehydration-induced changes in pressure–volume relationships of *Artemisia tridentata* Nutt. ssp. *tridentata*. Plant Cell Environ. 13:455–461.

Fisher, R.A., M. Williams, R. Lobo do Vale, A. Lola Da Costa and P. Meir. 2006. Evidence from Amazonian forests is consistent with isohydric control of leaf water potential. Plant Cell Environ. 29:151–165.

Gartner, B.L. and F.C. Meinzer. 2005. Structure–function relationships in sapwood water transport and storage. *In* Vascular Transport in Plants. Eds. N.M. Holbrook and M.A. Zwieniecki. Elsevier, Boston, MA, pp 307–331.

Goldstein, G., J.L. Andrade, F.C. Meinzer, N.M. Holbrook, J. Cavelier, P. Jackson and A. Celis. 1998. Stem water storage and diurnal patterns of water use in tropical forest canopy trees. Plant Cell Environ. 21:397–406.

Granier, A. 1985. Une nouvelle méthode pour la mesure de flux de sève brute dans le tronc des arbres. Ann. Sci. Forest. 42:193–200.

Hacke, U.G., J.S. Sperry, W.T. Pockman, S.D. Davis and K.A. McCulloh. 2001. Trends in wood density and structure are linked to prevention of xylem implosion by negative pressure. Oecologia 126:457–461.

Hubbard, R.M., M.G. Ryan, V. Stiller and J.S. Sperry. 2001. Stomatal conductance and photosynthesis vary linearly with plant hydraulic conductance in ponderosa pine. Plant Cell Environ. 24:113–121.

James, S.A., M.J. Clearwater, F.C. Meinzer and G. Goldstein. 2002. Variable length heat dissipation probes for the measurement of sap flow in trees with deep sapwood. Tree Physiol. 22:277–283.

Küppers, M. 1984. Carbon relations and competition between woody species in a central European hedgerow II. Stomatal responses, water use and hydraulic conductivity in the root/leaf pathway. Oecologia 64:344–354.

McDowell, N., H. Barnard, B.J. Bond et al. 2002*a*. The relationship between tree height and leaf area:sapwood area ratio. Oecologia 132:12–20.

McDowell, N.G., N. Phillips, C. Lunch, B.J. Bond and M.G. Ryan. 2002*b*. An investigation of hydraulic limitation and compensation in large, old Douglas-fir trees. Tree Physiol. 22:763–774.

Meinzer, F.C. 2002. Co-ordination of liquid and vapor phase water transport properties in plants. Plant Cell Environ. 25:265–274.

Meinzer, F.C. 2003. Functional convergence in plant responses to the environment. Oecologia 134:1–11.

Meinzer, F.C. and D.A. Grantz. 1990. Stomatal and hydraulic conductance in growing sugarcane: stomatal adjustment to water transport capacity. Plant Cell Environ. 13:383–388.

Meinzer, F.C., P.W. Rundel, M.R. Sharifi and E.T. Nilsen. 1986. Turgor and osmotic relations of the desert shrub *Larrea tridentata*. Plant Cell Environ. 9:467–475.

Meinzer, F.C., G. Goldstein, P.J. Jackson, N.M. Holbrook and M.V. Gutierrez. 1995. Environmental and physiological regulation of transpiration in tropical forest gap species: the influence of boundary layer and hydraulic properties. Oecologia 101:514–522.

Meinzer, F.C., S.A. James, G. Goldstein and D. Woodruff. 2003. Whole-tree water transport scales with sapwood capacitance in tropical forest canopy trees. Plant Cell Environ. 26:1147–1155.

Meinzer, F.C., D.R. Woodruff and D.C. Shaw. 2004. Integrated responses of hydraulic architecture, water and carbon relations of western hemlock to dwarf mistletoe infection. Plant Cell Environ. 27:937–946.

Meinzer, F.C., D.R. Woodruff, J.-C. Domec, G. Goldstein, P.I. Campanello, M.G. Gatti and R. Villalobos-Vega. 2008. Coordination of leaf and stem water transport properties in tropical forest trees. Oecologia 156:31–41.

Mencuccini, M. 2003. The ecological significance of long-distance water transport: short-term regulation, long-term acclimation and the hydraulic costs of stature across plant life forms. Plant Cell Environ. 26:163–182.

Muller-Landau, H.C. 2004. Interspecific and inter-site variation in wood specific gravity of tropical trees. Biotropica 36:20–32.

Pratt, R.B., A.L. Jacobsen, F.W. Ewers and S.D. Davis. 2007. Relationships among xylem transport, biomechanics and storage in stems and roots of nine Rhamnaceae species of the California chaparral. New Phytol. 174:787–798.

Rascher, U., M. Liebig and U. Lüttge. 2000. Evaluation of instant light-response curves of chlorophyll fluorescence parameter obtained with portable chlorophyll fluorometer on site in the field. Plant Cell Environ. 23:1397–1405.

Santiago, L.S., G. Goldstein, F.C. Meinzer, J.B. Fisher, K. Machado, D. Woodruff and T. Jones. 2004. Leaf photosynthetic traits scale with hydraulic conductivity and wood density in Panamanian forest canopy trees. Oecologia 140:543–550.

Scholz, F.G., S.J. Bucci, G. Goldstein, F.C. Meinzer, A.C. Franco and F. Miralles-Wilhelm. 2007. Biophysical properties and functional significance of stem water storage tissues in neo-tropical savanna trees. Plant Cell Environ. 30:236–248.

Sperry, J.S., U.G. Hacke, R. Oren and J.P. Comstock. 2002. Water deficits and hydraulic limits to leaf water supply. Plant Cell Environ. 25:251–263.

Stratton, L., G. Goldstein and F.C. Meinzer. 2000. Stem water storage capacity and efficiency of water transport: their functional significance in a Hawaiian dry forest. Plant Cell Environ. 23:99–106.

Suzuki, E. 1999. Diversity in specific gravity and water content of wood among Bornean tropical rain forest trees. Ecol. Res. 14:211–224.

Tausend, P.C., G. Goldstein and F.C. Meinzer. 2000. Control of transpiration in three coffee cultivars: the role of hydraulic and crown architecture. Trees 14:181–190.

Tyree, M.T. and H.T. Hammel. 1972. The measurement of the turgor pressure and water relations of plants by the pressure bomb technique. J. Exp. Bot. 23:267–282.

Van Gelder, H.A., L. Poorter and F.J. Sterck. 2006. Wood mechanics, allometry and life-history variation in a tropical rain forest tree community. New Phytol. 171:367–378.

Wright, I.J., D.S. Falster, M. Pickup and M. Westoby. 2006. Cross-species patterns in the coordination between leaf and stem traits, and their implications for plant hydraulics. Physiol. Plant. 127:445–456.